

Multiport bidirectional converter for solar fed hybrid electric vehicle using switched reluctance motor drive

Sivaprasad Kollati¹, Satish Kumar Gudey²

¹Andhra University Trans-Disciplinary Research Hub, Department of Electrical Engineering, Andhra University, Visakhapatnam, India

²Department of Electrical Engineering, Gayatri Vidya Parishad College of Engineering (Autonomous), Visakhapatnam, India

Article Info

Article history:

Received Sep 16, 2023

Revised Feb 15, 2024

Accepted Mar 12, 2024

Keywords:

(n+1) diode (n+1)

8/6 SRM

KY converter

PI controller

PV panel

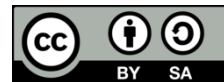
PWM generator

Semiconductor topology

ABSTRACT

For use in solar-assisted hybrid electric vehicle applications, a multiport bidirectional switched reluctance motor (SRM) drive is suggested in this research. Since the photovoltaic (PV) system's output voltage is low and insufficient to reach the necessary voltage level, a high gain KY converter is used to increase the PV output. The 8/6 SRM receives the steady converter output via the (n+1) diode (n+1) converter architecture with the help of the proportional integral (PI) controller. A PI controller regulates the SRM's speed. A bidirectional battery converter connects the battery, which is attached to the DC bus, to the extra power from the PV. A PI controller manages the bidirectional battery converter's operations. When necessary, the battery transfers the excess energy from the PV to the SRM drive. The outcomes demonstrate that, when examined using MATLAB simulation, the recommended methodology functions well.

This is an open access article under the [CC BY-SA](#) license.



Corresponding Author:

Sivaprasad Kollati

Andhra University Trans-Disciplinary Research Hub, Department of Electrical Engineering

Andhra University

Visakhapatnam, Andhra Pradesh 530003, India

Email: ksivaprasad22@gmail.com

1. INTRODUCTION

Social progress and energy growth are intrinsically tied to human survival. The paradox that fossil fuel supplies are running out while energy use is rising arises from advances in science and technology [1], [2]. Hence there is always new crises and dilemmas encountered by us. The only option is to use renewable energy sources (RES) which are less abundant and are derived from naturally regenerated sources [3]. Due to the abundance of solar irradiance compared to other RES, solar photovoltaic (PV) systems have recently played an important role in renewable energy systems (RESs) [4].

Solar energy [5] is uncontaminated and emits no pollutants once installed. They have numerous advantages, including unlimited access and being inexpensive. Additionally, solar energy generates an energy output that is more stable than wind energy. Solar farms are built on the roofs of buildings like homes or offices and are used to generate electricity on a large scale. They don't need a separate installation site. There are two ways to use the solar framework: off-grid (stand-alone) and grid-connected. Applying various DC-DC converters, such as boost [6], single-ended primary-inductance converter (SEPIC) [7], and Cuk [8], improves the output of PV panels.

As advances in science and technology advance, people will inevitably encounter new problems and difficulties. One such problem is the conflict that exists between the growing need for energy and the finite supply of fossil fuels. The main goal of global energy development going forward is to solve the power shortage and reduce carbon emissions by creating new energy sources instead of relying on fossil fuels. The

energy problem in the transportation industry may be resolved by the use of electrical vehicles (EVs), which depend less on traditional sources of energy. EVs are a recent scientific breakthrough.

EVs are more fuel-efficient, and when energy costs are taken into account, charging an EV is less expensive than fueling a diesel or gasoline vehicle. By utilizing RES, EVs are made more environment friendly. As a result, many literature studies are being conducted to advance the overall efficiency of EVs while also lowering costs. But the issues with current EV technology include a short range, a high initial cost, and a lengthy recharging time. Many cities and developing nations may not find it problematic that EVs have a limited range. Even in these appropriate locations, there is now a barrier to admission due to the absence of fast-charging facilities. Hybrid EVs (HEVs) are one option for getting over the drawbacks of EVs [9], [10]. It is possible to create HEV technology to address the aforementioned EV drawbacks. The drawbacks of using various EV motors [11], [12] like induction motors (IMs), permanent magnet synchronous motor (PMSM), and switching reluctance motors (SRM) motors [13] like low cost, long range EVs and contemporary methods to overcome them have been discussed. The results show that SRM is found to be a better option due to its economic advantages. However, it creates a lot of commotion and fluctuations in torque, which makes it difficult for EVs to use.

To solve this problem, prime mover with induction motor (IM) [14], [15] SRM have been proposed. Induction motors were commonly utilized in solar EV system in the past. Permanent magnets and rotor windings are not present in SRMs, which are noted for their more robust and straightforward construction. SRMs are a viable alternative for HEVs due to a number of inherent advantages, including efficient operation and high initial torque during first accelerations [16], [17]. In an attempt to improve machine performance, a variety of novel SRM drive configurations and related control algorithms have been investigated [17], [18]. An integrated converter with three ports is shown, which can minimize the DC-link capacitance and reduce current ripple. Consequently, the SRM drive's price and volume can be lowered [19]. The SRM operates on the basis of the magneto resistance reducing principle in the previously specified driving topologies, in which the unsmooth unilateral square-wave energy drives the stator winding. Because of this, there is still a lot of torque ripple and vibration, which has a negative impact on how comfortable an EV is to drive [20], [21].

The key benefit of this arrangement is that DC motors may be linked directly to solar array. However, the system performance may not be optimal in this instance. As a result, a DC-DC converter might be used to efficiently drive the system. Induction motors are magnet less, so they are less expensive than PMSMs. IMs are only used for high power rating applications. The drawback of IM is that it cannot be used for low power applications. SRM is used in EVs over other types of electric motor because of its great efficiency and control flexibility [22]–[24]. The stability analysis of the controllers is done using state space analysis.

The SRM system incorporates several voltage enhancing converters to improve the horsepower of the motor and provide broad speed control. These converters are used to link the solar panel with the load and serve as an impedance matching device. In order to choose the best power converter, different types of DC-DC power converters have been explored. Buck-boost, Cuk, boost, and SEPIC converters are widely used DC-DC converters. These power converters are usually integrated with maximum power point tracking (MPPT) controller [25]. In SRM-based HEV system a cascaded multiport converter has been proposed. This converter provides flexible energy conversion. However, switching losses prevent the proposed system from becoming more efficient. An incremental conductance (InC) approach to extracting peak power from solar system is presented. The light electric vehicles (LEVs) driving range has been improved. However, the system optimization is lacking.

In this work, a multi-port bidirectional SRM drive for solar based hybrid EV is proposed. A high gain KY converter is incorporated into the circuit. To increase PV voltage, the resultant power of the PV panel is linked to the KY converter. As a result, the drive input voltage is increased and the fluctuations of voltage are also minimized. The proposed system is validated using MATLAB simulation.

2. DEVELOPED SYSTEM USING A PROPORTIONAL INTEGRAL (PI) CONTROLLER

The process of enhancing the speed control of the SR motor in driving the electrical vehicle using (n+1) diode (n+1) semiconductor topology is introduced in this work and Figure 1 shows a block schematic that develops the system's operation. Considering that PV systems are sporadic, a low output voltage is obtained. Hence a KY converter is used to boost the voltage with good voltage regulation. The switching pulses are generated at a switching frequency of 1 MHz. To stabilize the converter voltage a PI controller is utilized resulting in a regulated output voltage. The converter output is given to the SR motor without any disruptions whereas the motor speed is controlled by comparing N_{act} and N_{ref} with PI controller. A bidirectional battery conversion that operates simultaneously in buck and boost modes stores the extra power from PV cells in a battery. This reduces power loss and motor power shortages, which improves

system performance throughout a larger range without requiring any complicated adjustments. Moreover, the battery operation gets tuned by the implementation of the PI controller in an efficient manner.

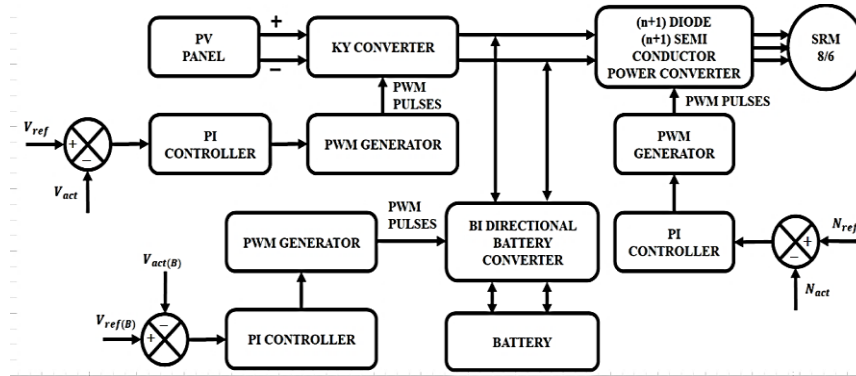


Figure 1. Block schematic for the suggested system

3. SYSTEM MODELLING

The design and operational measures of components used in this system are remarkably explained in the subsequent section with detailed analysis. The solar PV system and the KY converter is explained in detail as follows. Mathematical expressions related to SR motor are derived and the design of PI controller is also described in this section.

3.1. Solar PV system

The best-known application of PV is to generate electricity by engaging solar cells to transform solar energy into electron flow through the PV effect. Solar cells utilize sunlight to produce DC electricity that runs devices or recharges batteries. The current source I_{PH} in the equivalent circuit of PV is parallel connected to the diode D as portrayed in Figure 2 in which R_S and R_{SH} represents series and shunt resistance respectively. In general, R_{SH} is too large whereas R_S is too small.

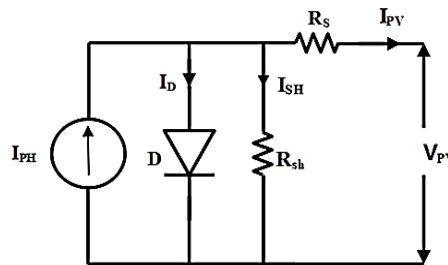


Figure 2. Equivalent PV system circuit

The mathematical expression of the voltage and current is basically expressed as (1). Here, the cell temperature is taken as T , parallel connected cells count is represented as N_p , series resistance is signified as R_S , the photo current is detailed as I_{PH} , series connected cells count is signified as N_s , A be the ideal factor, k is described as Boltzmann constant and saturation current of module is specified as I_S . The I_{PH} is linearly depended on solar irradiance and temperature, which is thus expressed as (2).

$$I_{PV} = N_p I_{PH} - N_p I_S \left[\exp \frac{q(V + I R_S)}{N_s k T A} - 1 \right] \quad (1)$$

$$I_{PH} = [I_{SC} + K_1(T - T_R)]\lambda \quad (2)$$

Here, solar irradiance range is indicated as λ , short circuit current as I_{SC} , reference temperature as T_R and temperature of short circuit current is indicated as K_1 . This results in the expression for reverse saturation current at reference temperature, shown as (3).

$$I_{RS} = \frac{I_{SC}}{\exp\left[\frac{qV_{OC}}{N_S kTA}\right]} \quad (3)$$

Here, the circuit voltage is indicated as V_{OC} . The obtained voltage of PV is then fed to the KY converter as input in an efficient manner.

3.2. KY converter

The significance of the KY converter in the process of maximizing PV output is extremely high as it has maximal transient response, high gain, improved efficiency and synchronous rectification. It involves enhancing the output voltage by minimizing the stress and ripples in the voltage. It is also capable of effectively compensating the load voltage. The circuit representation of a KY converter is illustrated in Figure 3. With its capacity to respond quickly in a transient, it maximizes PV output over a larger range. This converter's voltage gain is shown as (4).

$$M = \frac{V_o}{V_i} = 1 + D \quad (4)$$

By the slew rate of current that flows through L in no load condition SR_L , the output inductor is evaluated as (5).

$$SR_L = \frac{2V_i - V_o}{L} \quad (5)$$

Hence:

$$L = \frac{2V_i - V_o}{SR_L} \quad (6)$$

Here, output voltage is indicated as V_o , current through L is indicated as I and input voltage are indicated as V_o . Similarly, capacitor output is evaluated by considering the slew rate of output current in the rated load condition as (7).

$$C = \frac{\Delta Q}{\Delta V_C} \quad (7)$$

Here, the peak-peak voltage is taken as ΔV_C . Thus, the proposed converter performs well in improving low voltage of PV in an efficient manner, which in turn enhances the efficiency of the system performance.

3.3. (n+1) diode (n+1) semiconductor power converter

The obtained output of KY converter is applied to the SR motor through the suggested power converter. This implementation of this power converter topology is extremely beneficial since it extremely minimizes the cost and losses by having fewer switches, which significantly improves the disruption free operation of the system. For all the diodes and switching devices, the voltage rating V_{dc} is small and the circuit illustration of this topology is significantly highlighted in Figure 4 to enhance the operation of the power converter in an efficient manner. The circuit includes four diodes (D, D_1, D_2 , and D_3), four switches (T_1, T_2, T_3 , and T_4) and four phase windings (A, B, C , and D), which are illustrated in the subsequent figure.

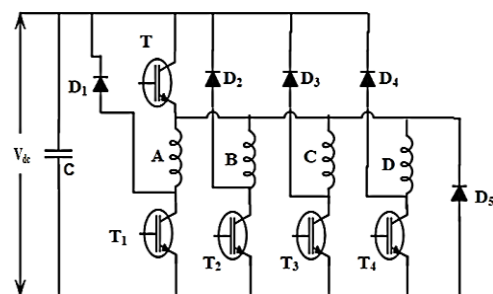
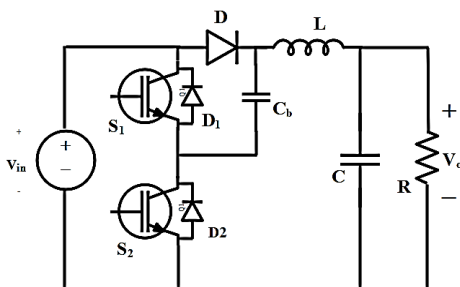


Figure 3. Circuit diagram of a KY converter Figure 4. (n+1) diode (n+1) semiconductor power converter

As specified in Figure 4, it employs less diodes and power switches. From the DC source, the phase winding A gets energized during ON condition of switches T and T_1 whereas the stored energy in windings

phase, A is returned to mains via D and D_1 during the OFF condition of switches T and T_1 . B gets energised during the ON condition of switches T and T_2 whereas the stored energy in B gets returned to mains via D and D_2 during the OFF condition of switches T and T_2 . Through D and D_3 , the preserved energy in winding C is returned to the mains when the switches T and T_3 are opened whereas the winding C is charged when T and T_3 are closed. Similarly, the conserved energy in winding D is returned to the mains through D and D_4 when T and T_4 are opened but it gets charged when the switches T and T_4 are closed. The attained output of this power converter is the fed to the SR motor as the input. Where are the output terminals in the KY converter Figure 4.

3.4. Expressions related to SR motor

The implementation of a 4Φ SR motor with 8/6 stator and rotor poles is preferred in this present work for driving the electric vehicle. In this motor, all the phases are identical and the common inductance among the phases is ignored. In accordance with the time, the voltage given to the phase is expressed as (8) and (9).

$$V = R_s i + \frac{d\psi(\theta, i)}{dt} \quad (8)$$

$$\psi = L(\theta, i) i \quad (9)$$

Here ψ and R_s signify the flux linkage and resistance per phase whereas L signifies the inductance. Phase voltages is expressed in terms of the inductance as (10).

$$\begin{aligned} V &= R_s i + \frac{d\{L(\theta, i)i\}}{dt} \\ V &= R_s i + L(\theta, i) \frac{di}{dt} + i \omega \frac{dL(\theta, i)}{d\theta} \end{aligned} \quad (10)$$

The subsequent equation specifies the induced EMF as (11) and (12).

$$e = \frac{dL(\theta, i)}{d\theta} \omega_m i = k_b \omega_m i \quad (11)$$

EMF constant:

$$k_b = \frac{dL(\theta, i)}{d\theta} \quad (12)$$

the SR motor's equivalent circuit representation is remarkably depicted in Figure 5 in an efficient manner.

The following expression specifies the Instantaneous input current as (13) and (14).

$$P_i = R_s i^2 + i^2 \frac{dL(\theta, i)}{dt} + L(\theta, i) i \frac{di}{dt} \quad (13)$$

$$\frac{d}{dt} \left(\frac{1}{2} L(\theta, i) i^2 \right) = L(\theta, i) i \frac{di}{dt} + \frac{1}{2} i^2 \frac{dL(\theta, i)}{dt} \quad (14)$$

Substitute (14) is obtained as (13) and (15).

$$P_i = R_s i^2 + \frac{d}{dt} \left(\frac{1}{2} L(\theta, i) i^2 + \frac{1}{2} i^2 \frac{dL(\theta, i)}{dt} \right) \quad (15)$$

Here, the resistive loss is indicated as P_i . The rate of air gap power and changes in field energy is indicated as P_a .

$$P_a = \frac{1}{2} i^2 \frac{dL(\theta, i)}{dt} \quad (16)$$

By considering the time, it is specified as (17).

$$\begin{aligned} P_a &= \frac{1}{2} i^2 \frac{dL(\theta, i)}{dt} = \frac{1}{2} i^2 \frac{dL(\theta, i)}{d\theta} \cdot \frac{d\theta}{dt} \\ P_a &= \frac{1}{2} i^2 \frac{dL(\theta, i)}{d\theta} \omega_m \end{aligned} \quad (17)$$

Thus, the product of rotor speed and torque is mentioned as P_a , which is as in (18).

$$P_a = \omega_m T_e \quad (18)$$

Therefore, the SR motor functions well in operating the electric vehicle in an efficient manner which is validated through analysis of the before mentioned formations.

3.5. Design of PI controller

The role that a PI controller provides in regulating output from the converter, SR motor speed and battery operation are significantly high in this present work as it analyzes the carrier signal with the reference signal and generates the optimized output in an enhanced way. The block illustration of this PI controller is presented in Figure 6. The PI controller produces the error sign as its output and this controller produces output signal $u(t)$ with two levels like integral of input signal and input signal $e(t)$. Moreover, it involves in minimizing steady state error. The error and output signal of the controller are equivalent to each other which is obtained as (19) and (20).

$$u(t) \propto [e(t) + \int e(t)dt] \quad (19)$$

$$u(t) = K_p e(t) + K_i \int e(t)dt \quad (20)$$

Here, $K_i = \cos \frac{\theta}{A_1}$ indicates integral gain and $K_p = -\omega_1 \sin \frac{\theta}{A_1}$ indicates proportional gain. The transfer function of this PI controller is thus mentioned as (21).

$$G_c(s) = \frac{U(s)}{E(s)} = \frac{K_p + K_i}{s} \quad (21)$$

Therefore, it is evaluated that a PI controller is highly efficient in controlling converter, motor and battery control parameters.

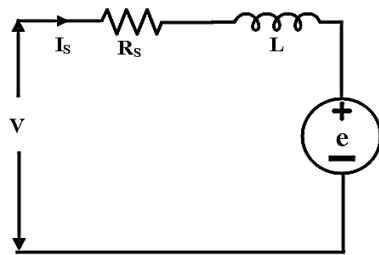


Figure 5. Equivalent circuit of SR motor

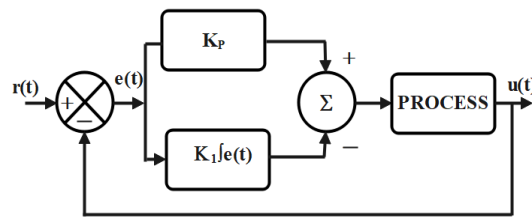


Figure 6. Representation of PI controller

3.6. Charging and discharging circuit of a battery

The bidirectional battery converter is employed to lessen the wastage and shortage of power supply since it operates in both the buck and boost modes for regulating power flow control. It is highly advantageous in lessening the interruptions in the operation of the system without any complexities since it retains the optimal value of DC link voltage in an efficient manner. The power flow in a bidirectional way is significantly illustrated through the circuit representation in Figure 7. The battery discharges the power through the inductor to the motor during the discharging mode whereas the battery gets charged from the inductor during the charging mode, which in turn enhances the cumulative performance of the system in the process of driving the electric vehicle without any interruptions. Thus, the contribution of this battery converter is highly advantageous.

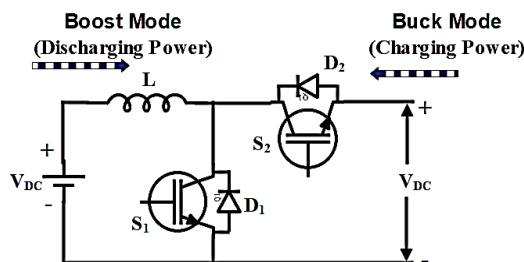


Figure 7. Charging and discharging circuit for bidirectional power flow of a battery

4. RESULTS AND DISCUSSIONS

In this study, a multi-port bidirectional SRM drive for solar-powered HEV applications is described. The parameters of SRM motor and PV panel are given in Tables 1 and 2, respectively. MATLAB/Simulink is used to simulate the suggested work, and the associated outcomes are achieved. Initially a reference voltage of 600 V is maintained by the converter, which is further enhanced and stabilized with the support controller approach. In contrast a 1500 rpm is assigned to be the reference speed which is operating at a switching frequency of 1 MHz. The switching pulses are generated based on the switching frequency applied to the system. The configuration characteristics of the PV system under examination are displayed in Table 1.

Table 1. Parameter specifications of solar panel

S.L.	Parameters	Values
1	Peak power current (I_{mp})	5.42 A
2	Short circuit current (I_{sc})	5.86 A
3	Peak power voltage (V_{mp})	18.75 V
4	Quantity of series-connected cells (N_s)	36
5	Open circuit voltage (V_{oc})	22.68 V
6	Peak power (P_{mp})	8 KW, 16 Panels

Table 2. Parameter specifications of SRM

S.L.	Parameters	Values	S.L.	Parameters	Values
1	Motor rating (Hp)	1 Hp	6	Rotor inertia	0.1 lb-ft ²
2	Supply voltage (V)	230 V AC (rms)	7	Peak system efficiency(η)	91%
3	Rated speed (rpm)	3600 rpm	8	Insulation class	F
4	Number of phases	4	9	Current (I)	3.24 A
5	Supply frequency (f)	50 Hz			

4.1. Determination of stability

Utilizing a combination of feedback, frequency response analyses have been utilized to examine the stability of the KY converter's control system. The transfer functions derived from state space models are used to generate the frequency response plots. It is possible to derive the transfer function from an open loop of the system using the state space model. The open loop transmit factor can be seen in (22).

$$G(s) = c(sI - A)^{-1}b \quad (22)$$

When switch Q_1 is ON and Q_2 is in OFF state, the voltage equation becomes (23).

$$-V_{dc} + L \frac{di}{dt} + V_o = 0 \quad (23)$$

On neglecting voltage drop across capacitor C_b , the equation becomes (24) and (25).

$$\frac{dI}{dt} = \frac{V_{dc}}{L} - \frac{V_o}{L} \quad (24)$$

$$I = \frac{V_{dc}}{L} - \frac{V_o}{L} \quad (25)$$

The formula yields the current flowing through capacitor C.

$$i_c = C \cdot \frac{dV_o}{dt}$$

$$\frac{dV_o}{dt} = \frac{1}{C} \cdot i_c = \frac{1}{C} (-I_L + I) \quad (26)$$

$$V_o = -\frac{1}{C} \cdot \frac{V_o}{R} + \frac{I}{C} \quad (27)$$

$$\begin{bmatrix} I \\ V_o \end{bmatrix} = \begin{bmatrix} 0 & \frac{-1}{L} \\ \frac{1}{C} & \frac{-1}{Rc} \end{bmatrix} \begin{bmatrix} I \\ V_o \end{bmatrix} + \begin{bmatrix} \frac{V_{dc}}{L} \\ 0 \end{bmatrix} \quad (28)$$

$$r = [1 \ 1] \begin{bmatrix} I \\ V_o \end{bmatrix}; A = \begin{bmatrix} 0 & \frac{-1}{L} \\ \frac{1}{C} & \frac{-1}{RC} \end{bmatrix}; B = \begin{bmatrix} \frac{V_{dc}}{L} \\ 0 \end{bmatrix} \text{ and } C = [1 \ 1] \quad (29)$$

The stability of a certain feedback control system is assessed using an open loop transfer function Bode plot. Table 3 lists the system parameters for KY converter circuit that are taken into consideration for analysis. Figure 8 represents the classical controller approach.

By using state feedback approach the results are obtained for the output matrix $C = [1 \ 1]$ respectively. Figure 9 shows the matching frequency response plot. While the phase margin has a value of 1.9 degrees, the gain margin has an infinite value. Hence the system is said to be stable using a PI controller with the control parameters V_o and I .

Table 3. Parameters of KY converter

S.L.	Parameters	Values
1	DC link voltage (V_{dc})	16 V
2	Output voltage (V_o)	24 V
3	Switching frequency (f_s)	10 kHz
4	Output power (P_o)	0.1 kW
5	Inductor (L)	8 μ H
6	Capacitor (C)	850 μ F

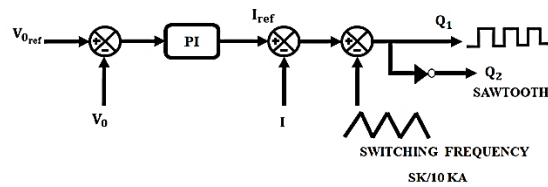


Figure 8. Classical PI controller

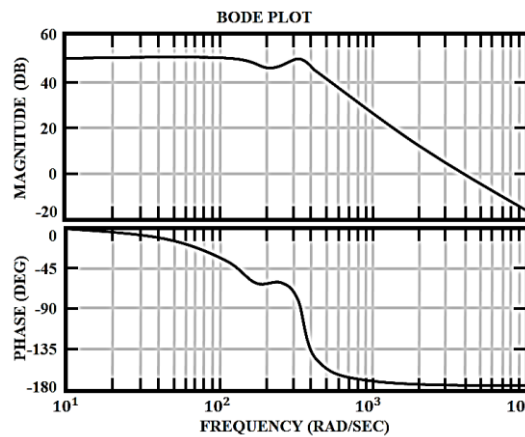


Figure 9. Frequency response plot of the open loop transfer characteristic of the KY converter circuit

4.2. Simulation results

The results obtained using MATLAB/Simulink for the proposed work are as follows: The main objective of the proposed simulation shown in Figure 10 is to provide a constant supply for the uninterrupted functioning of the SR motor. The PV output is applied to the converter to generate an increased DC voltage. The gain parameters for the PI controller are selected as shown in Table 4 for the efficient functioning of the converter. The obtained DC link voltage is used for energizing the SR motor. The SOC of the battery is maintained at a specific level which when increased, can be used to energize the motor.

Table 4. PI controller parameters

S.L.	Parameters	Values
1	Proportional gain (K_p)	0.1
2	Integral gain (K_i)	0.01

The switching pulse obtained from the PWM generator is indicated in Figure 11. In order to ensure that the KY converter operates well, continuous signals are given to its relays via the PI controller, which also helps to regulate the PWM generator. Figure 12 denotes the waveform for battery SOC which indicates a charge level of 80%. The DC link receives the extra energy generated by the battery to power the SR motor.

The back EMF waveform of the SRM is given in Figure 13. The waveform initially has fluctuations and then it stabilizes from 0.15 s at the constant value of about 120 V. From 0.6 s, the back EMF of the SRM is 140 V. The current waveform of the SRM is given in Figure 14. The current rapidly varies up to 0.15 s and then it stabilizes at around 0.3 s and reaches the value of 5 A.

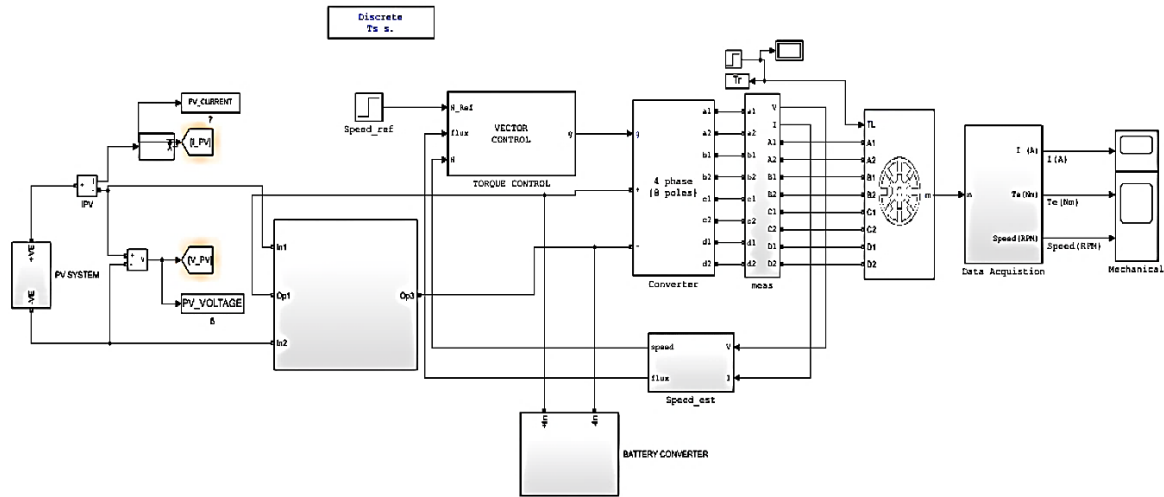


Figure 10. Simulation diagram

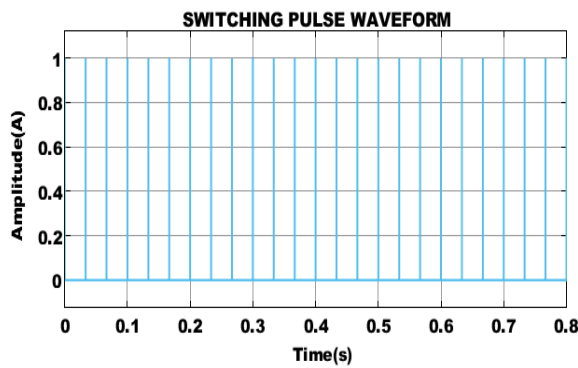


Figure 11. Switching pulses to the converter

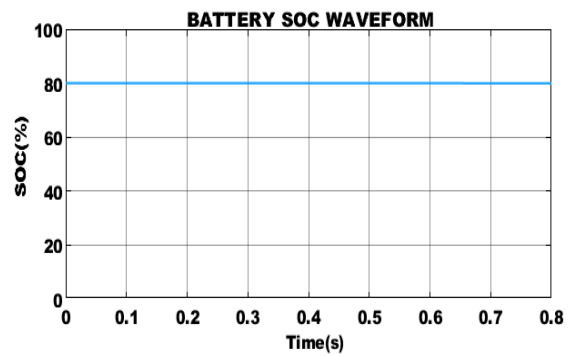


Figure 12. Waveform of the battery SOC

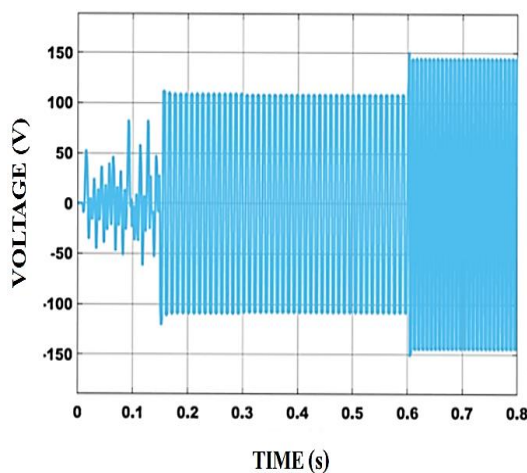


Figure 13. Motor back EMF waveform

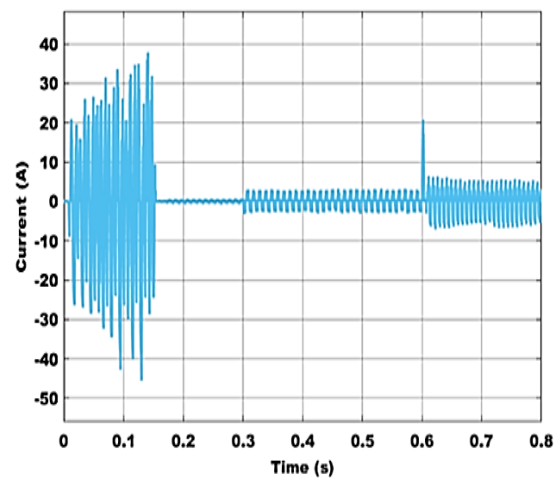


Figure 14. Motor current waveform

Figure 15 depicts the motor's speed waveform. Initially, the reference speed is maintained at 1500 rpm and it reaches 2000 rpm at 0.6 s. The actual speed of the SRM shows fluctuations at the beginning and becomes stable after 0.15 s. The torque waveform of the SRM is displayed in Figure 16. The torque of the motor fluctuates initially till 0.15 s and reaches the value of 5 Nm at 0.3 s.

Figure 17 shows the graphical representation of efficiency for converters such as boost, Cuk, SEPIC, and the planned KY converter. From Figure 17, it is observed that boost converter attains the lowest efficiency of 90% followed by Cuk and SEPIC converter with 91.2% and 92.38% efficiency. However, the maximum efficiency of 94.8% is attained by the proposed KY converter. Figure 18 shows the voltage gain that various converters may achieve. In contrast to current converters such as boost, Cuk, and SEPIC, which yield gain values of 1:1.5, 1:3, and 1:8, the KY converter proposed in this work reaches a high peak voltage rise of 1:10. Settling time attained using various converters in comparison with proposed KY converter is depicted in Figure 19. It is observed that KY converter shows best settling time of 0.65 s, in contrast to other converters like boost, Cuk, and SEPIC settles at 0.89 s, 0.81 s, and 0.78 s respectively.

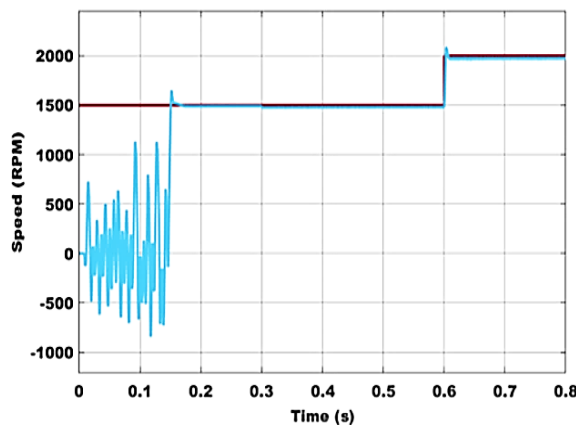


Figure 15. Motor speed waveform

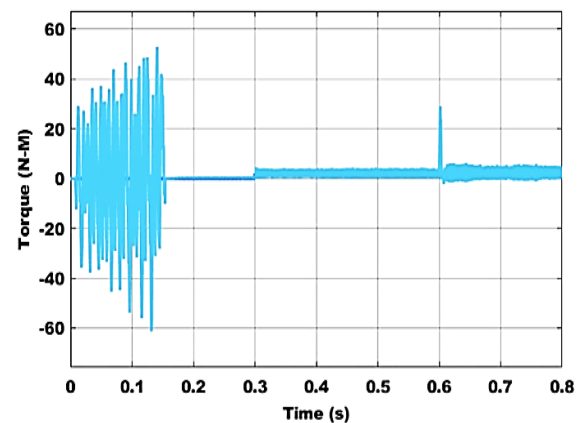


Figure 16. Motor torque waveform

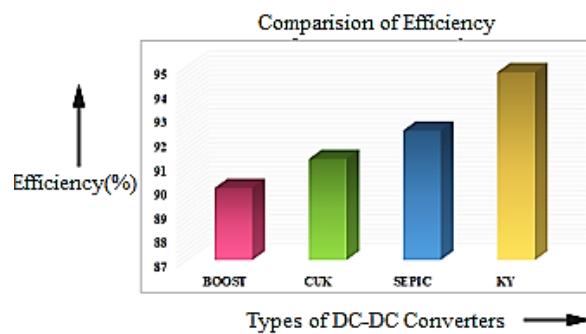


Figure 17. Comparison of efficiency

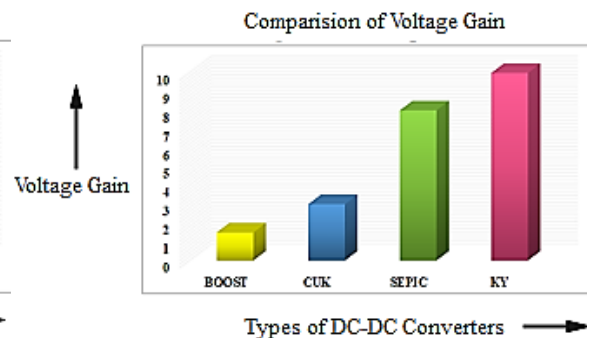


Figure 18. Voltage gain comparison

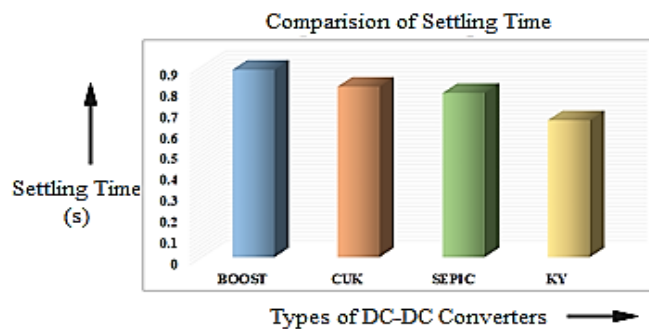


Figure 19. Comparison of settling time using converter

5. CONCLUSION

The increasing need for electrical power, the diminishing reserves of fossil fuels, and the negative effects of rising temperatures have made the development of a clean and sustainable power generation and transportation system imperative. This research proposes a multi-port bidirectional SRM drive for solar-based HEV applications. Utilizing a high gain KY converter, the PV output is raised since the system voltage is low and unable to supply the required voltage. Using a $(n+1)$ diode $(n+1)$ circuit design, the converter output is routed to the 8/6 SRM with the assistance of a PI controller to ensure its stability. In order to control SRM speed, a PI controller is employed. A bidirectional battery converter connects the battery to the DC bus, serving as a supplemental supply. A PI controller regulates both the bidirectional battery converter's boost and buck modes of operation. Lastly, the effective functioning of the suggested system is confirmed through the use of the MATLAB simulation.




REFERENCES

- [1] A. Bharatee, P. K. Ray, and A. Ghosh, "A power management scheme for grid-connected PV integrated with hybrid energy storage system," *Journal of Modern Power Systems and Clean Energy*, vol. 10, no. 4, pp. 954–963, 2022, doi: 10.35833/MPCE.2021.000023.
- [2] E. Du *et al.*, "The role of concentrating solar power toward high renewable energy penetrated power systems," *IEEE Transactions on Power Systems*, vol. 33, no. 6, pp. 6630–6641, Nov. 2018, doi: 10.1109/TPWRS.2018.2834461.
- [3] M. M. G. Lawan, J. Raharijaona, M. B. Camara, and B. Dakyo, "Power control for decentralized energy production system based on the renewable energies — using battery to compensate the wind/load/PV power fluctuations," in *2017 IEEE 6th International Conference on Renewable Energy Research and Applications (ICRERA)*, Nov. 2017, pp. 1132–1138, doi: 10.1109/ICRERA.2017.8191230.
- [4] D. van der Meer, G. R. Chandra Mouli, G. Morales-Espana Mouli, L. R. Elizondo, and P. Bauer, "Energy management system with PV power forecast to optimally charge EVs at the workplace," *IEEE Transactions on Industrial Informatics*, vol. 14, no. 1, pp. 311–320, Jan. 2018, doi: 10.1109/TII.2016.2634624.
- [5] S. Comello, S. Reichelstein, and A. Sahoo, "The road ahead for solar PV power," *Renewable and Sustainable Energy Reviews*, vol. 92, pp. 744–756, Sep. 2018, doi: 10.1016/j.rser.2018.04.098.
- [6] K. A. Singh, A. Prajapati, and K. Chaudhary, "High-gain compact interleaved boost converter with reduced voltage stress for PV application," *IEEE Journal of Emerging and Selected Topics in Power Electronics*, vol. 10, no. 4, pp. 4763–4770, Aug. 2022, doi: 10.1109/JESTPE.2021.3120802.
- [7] R. Bauwelz Gonzatti, Y. Li, M. Amirabadi, B. Lehman, and F. Z. Peng, "An overview of converter topologies and their derivations and interrelationships," *IEEE Journal of Emerging and Selected Topics in Power Electronics*, vol. 10, no. 6, pp. 6417–6429, Dec. 2022, doi: 10.1109/JESTPE.2022.3181217.
- [8] J. C. dos S. de Moraes, J. L. dos S. de Moraes, and R. Gules, "Photovoltaic AC module based on a Cuk converter with a switched-inductor structure," *IEEE Transactions on Industrial Electronics*, vol. 66, no. 5, pp. 3881–3890, May 2019, doi: 10.1109/TIE.2018.2856202.
- [9] M. Ehsani, K. V. Singh, H. O. Bansal, and R. T. Mehriardi, "State of the art and trends in electric and hybrid electric vehicles," *Proceedings of the IEEE*, vol. 109, no. 6, pp. 967–984, Jun. 2021, doi: 10.1109/JPROC.2021.3072788.
- [10] Y. Wang, H. Tan, Y. Wu, and J. Peng, "Hybrid electric vehicle energy management with computer vision and deep reinforcement learning," *IEEE Transactions on Industrial Informatics*, vol. 17, no. 6, pp. 3857–3868, Jun. 2021, doi: 10.1109/TII.2020.3015748.
- [11] Z. Wang, T. W. Ching, S. Huang, H. Wang, and T. Xu, "Challenges faced by electric vehicle motors and their solutions," *IEEE Access*, vol. 9, pp. 5228–5249, 2021, doi: 10.1109/ACCESS.2020.3045716.
- [12] H. Cheng, Z. Wang, S. Yang, J. Huang, and X. Ge, "An integrated SRM powertrain topology for plug-in hybrid electric vehicles with multiple driving and onboard charging capabilities," *IEEE Transactions on Transportation Electrification*, vol. 6, no. 2, pp. 578–591, Jun. 2020, doi: 10.1109/TTE.2020.2987167.
- [13] H.-C. Chen, W.-A. Wang, and B.-W. Huang, "Integrated driving/charging/discharging battery-powered four-phase switched reluctance motor drive with two current sensors," *IEEE Transactions on Power Electronics*, vol. 34, no. 6, pp. 5019–5022, Jun. 2019, doi: 10.1109/TPEL.2018.2880259.
- [14] J. Su, R. Gao, and I. Husain, "Model predictive control-based field-weakening strategy for traction EV used induction motor," *IEEE Transactions on Industry Applications*, vol. 54, no. 3, pp. 2295–2305, May 2018, doi: 10.1109/TIA.2017.2787994.
- [15] D. Ronanki and S. S. Williamson, "A simplified space vector pulse width modulation implementation in modular multilevel converters for electric ship propulsion systems," *IEEE Transactions on Transportation Electrification*, vol. 5, no. 1, pp. 335–342, Mar. 2019, doi: 10.1109/TTE.2018.2884610.
- [16] C. Gan, J. Wu, Y. Hu, S. Yang, W. Cao, and J. M. Guerrero, "New integrated multilevel converter for switched reluctance motor drives in plug-in hybrid electric vehicles with flexible energy conversion," *IEEE Transactions on Power Electronics*, vol. 32, no. 5, pp. 3754–3766, May 2017, doi: 10.1109/TPEL.2016.2583467.
- [17] Z. Yu, C. Gan, K. Ni, Y. Chen, and R. Qu, "Dual-electric-port bidirectional flux-modulated switched reluctance machine drive with multiple charging functions for electric vehicle applications," *IEEE Transactions on Power Electronics*, vol. 36, no. 5, pp. 5818–5831, May 2021, doi: 10.1109/TPEL.2020.3029822.
- [18] T. Wu, W. Li, K. Ni, S. Song, and M. Alkahtani, "Modular Tri-port converter for switched reluctance motor-based hybrid electrical vehicles," *IEEE Access*, vol. 7, pp. 15989–15998, 2019, doi: 10.1109/ACCESS.2019.2894818.
- [19] Q. Sun, J. Wu, C. Gan, J. Si, J. Guo, and Y. Hu, "Cascaded multiport converter for SRM-based hybrid electrical vehicle applications," *IEEE Transactions on Power Electronics*, vol. 34, no. 12, pp. 11940–11951, Dec. 2019, doi: 10.1109/TPEL.2019.2909187.
- [20] V. Shah and S. Payami, "An integrated driving/charging four-phase switched reluctance motor drive with reduced current sensors for electric vehicle application," *IEEE Journal of Emerging and Selected Topics in Power Electronics*, vol. 10, no. 6, pp. 6880–6890, Dec. 2022, doi: 10.1109/JESTPE.2021.3120468.
- [21] Q. Sun, H. Xie, X. Liu, F. Niu, and C. Gan, "Multiport PV-assisted electric-drive-reconstructed bidirectional charger with G2V and V2G/V2L functions for SRM drive-based EV application," *IEEE Journal of Emerging and Selected Topics in Power Electronics*, vol. 11, no. 3, pp. 3398–3408, Jun. 2023, doi: 10.1109/JESTPE.2023.3240434.




- [22] J. Cai and X. Zhao, "An on-board charger integrated power converter for EV switched reluctance motor drives," *IEEE Transactions on Industrial Electronics*, vol. 68, no. 5, pp. 3683–3692, May 2021, doi: 10.1109/TIE.2020.2982112.
- [23] X. Zan, G. Xu, T. Zhao, R. Wang, and L. Dai, "Multi-battery block module power converter for electric vehicle driven by switched reluctance motors," *IEEE Access*, vol. 9, pp. 140609–140618, 2021, doi: 10.1109/ACCESS.2021.3119782.
- [24] M. H. Mobarak, R. N. Kleiman, and J. Bauman, "Solar-charged electric vehicles: A comprehensive analysis of grid, driver, and environmental benefits," *IEEE Transactions on Transportation Electrification*, vol. 7, no. 2, pp. 579–603, Jun. 2021, doi: 10.1109/TTE.2020.2996363.
- [25] M. Ahmed, I. Harbi, R. Kennel, J. Rodriguez, and M. Abdelrahman, "Model-based maximum power point tracking algorithm with constant power generation capability and fast DC-link dynamics for two-stage PV systems," *IEEE Access*, vol. 10, pp. 48551–48568, 2022, doi: 10.1109/ACCESS.2022.3172292.

BIOGRAPHIES OF AUTHORS



Sivaprasad Kollati    is a research scholar, pursuing Ph.D., in Electrical Engineering at Andhra University, Visakhapatnam, Andhra Pradesh, India. He is in the field of Power Electronics and Renewable Energy Sources at Andhra University Trans-Disciplinary Research Hub, Andhra University, Visakhapatnam, Andhra Pradesh, India. He is working as an assistant professor in the Department of Electrical and Electronics Engineering at Godavari Institute of Engineering and Technology (Autonomous), Rajahmundry, Andhra Pradesh, India. He graduated in Electrical and Electronics Engineering at VIF College of Engineering and Technology, Hyderabad, India. He secured Master of Engineering in Power Electronics and Electric Drives at Pragati Engineering College, Surampalem, Andhra Pradesh, India. He is in teaching profession for more than 10 years. He has presented 14 papers in national and international journals, conference, and symposiums. His main area of interest includes power electronic and renewable energy systems. He can be contacted at email: ksivaprasad22@gmail.com.



Satish Kumar Gudey    received the B.Tech. degree in Electrical and Electronics Engineering from J.N.T.U. Hyderabad, Andhra Pradesh, India in 2000, then M.Tech. in Industrial Electrical systems from National Institute of Technology Durgapur, West Bengal, India, in 2002. He was awarded Doctor of Philosophy from Motilal Nehru National Institute of Technology Allahabad in the year 2015 in the area of Power Electronics. He has publications in reputed Journals like IET UK, Taylor and Francis, UK, IEEE USA. He is a regular reviewer of journal articles in IEEE transactions on Power Electronics, International journal of Electronics, Taylor and Francis, Elsevier Science. His research articles are well known in the area of power electronics with citations of around 321 with a h-index of 9. Presently he is working as a professor and HoD in the department of Electrical and Electronics Engineering (Autonomous), Gayatri Vidya Parishad College of Engineering (Autonomous), Visakhapatnam. His research interests include power electronics, distribution generation and applications of machine learning algorithms to power electronics systems. He is a Senior member of IEEE and a life member of ISTE, India. He has recently completed an AICTE project titled "Direct Torque Controlled Induction Motor Drive for Hybrid Electric Vehicles with Space Vector Modulated Sliding Mode Controller to Reduce Torque Ripple". The cost of project is 9 Lakhs. He can be contacted email: satishgudey5@gvpce.ac.in.